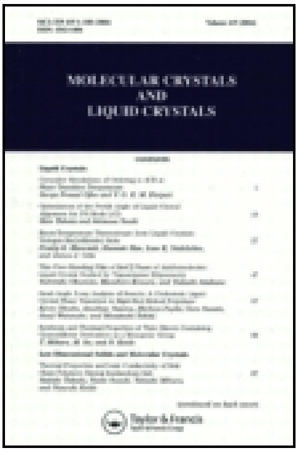

Molecular Crystals and Liquid Crystals Science and Technology. Section A. Molecular Crystals and Liquid Crystals

Publication details, including instructions for authors and subscription information:
http://www.tandfonline.com/loi/gmcl19

Director Distribution in Weakly Anchored Nematic Layers Deformed by Electric Fields

Grzegorz Derfel [a]

[a] Institute of Physics, Technical University of Łódź, ul. Wólczańska 223, 93-005, Łódź, Poland

Version of record first published: 23 Sep 2006.

Mol. Cryst. Liq. Cryst. 1995, Vol. 261, pp. 197–204
Reprints available directly from the publisher
Photocopying permitted by license only

DIRECTOR DISTRIBUTION IN WEAKLY ANCHORED NEMATIC LAYERS DEFORMED BY ELECTRIC FIELDS

GRZEGORZ DERFEL
Institute of Physics, Technical University of Łódź,
ul. Wólczańska 223, 93-005 Łódź, Poland.

Abstract The director deformations induced by electric field in weakly anchored nematic and chiral nematic layers were studied numerically. The director distributions were calculated for various parameters of the system, by minimizing the free energy in the course of an iterative process. The earlier qualitative results were confirmed.

INTRODUCTION

The weakly anchored nematic layers influenced by the electric fields have been studied theoretically in numerous works. In a previous paper[1], a method based on the catastrophe theory was applied to this problem. The deformations of the twisted (TN) and supertwisted (STN) planar nematic layers were described qualitatively due to the topological origin of the method. A variety of transitions between the twisted and the homeotropic states were revealed. In this paper, they are verified by means of numerical simulation of the director distribution.

In the system considered, the nematic material, characterized by the elastic constants k_{11}, k_{22}, and k_{33}, dielectric permittivities $\varepsilon_\perp$ and $\varepsilon_{||}$ and intrinsic pitch $P=2\lambda$, is confined between two electrodes, placed parallel to the (xy) plane at $z=\pm d/2$. The direction of the easy axis on the bottom surface is twisted in relation to that at the top surface by an angle Φ. The director distribution is determined by the angles $\theta(z)$ and $\omega(z)$, between the director and the (xy) and (yz) planes respectively. The total free energy per unit area of the layer is given by:

$$\begin{aligned} G = (k_{11}/2) \int_{-d/2}^{d/2} \Big[&(\cos^2\theta + k_b \sin^2\theta)(\partial\theta/\partial z)^2 \\ &+ \cos^2\theta (k_t \cos^2\theta + k_b \sin^2\theta)(\partial\omega/\partial z)^2 \\ &+ 2k_t(\pi/\lambda)\cos^2\theta(\partial\omega/\partial z) \Big] dz \\ &- \frac{U^2 \varepsilon_0 \Delta\varepsilon}{2\kappa \int_{-d/2}^{d/2} \frac{dz}{1+\kappa \sin^2\theta}} \\ &+ 2\gamma_1 \sin^2\psi + 2\gamma_2 \cos^2\psi \sin^2\delta \end{aligned} \quad (1)$$

where $k_b = k_{33}/k_{11}$, $k_t = k_{22}/k_{11}$, $\kappa = \Delta\varepsilon/\varepsilon_\perp$, $\Delta\varepsilon = \varepsilon_{||} - \varepsilon_\perp$, U is the applied voltage, γ_1 and γ_2 are the parameters that characterize the strength of the surface anchoring due to the surface tilt and twist respectively, $\psi = \theta(\pm d/2)$ and $\delta = \Phi/2 - |\omega(\pm d/2)|$.

METHOD

The numerical simulation applied in this work is analogous to the method used in other papers, for instance by Bedford and Windle[2]. The thickness of the layer is divided into N-1 sublayers by means of N equidistant planes. The polar and azimuthal angles, θ_i and ω_i respectively, are assigned to each plane. The total free energy per unit area of the layer, given by Eq. (1), is expressed as a function of these $2N$ angles. The variables $\theta(z)$ and $\omega(z)$ and their derivatives $d\theta/dz$ and $d\omega/dz$ are replaced by other quantities adopted for each sublayer. For the sublayer placed between the i-th and $(i+1)$-th planes, the suitable substitutions are: $\Theta_i = (\theta_i + \theta_{i+1})/2$, $\Omega_i = (\omega_i + \omega_{i+1})/2$, $\Theta_{i,z} = (\theta_{i+1} - \theta_i)(N-1)/d$, and $\Omega_{i,z} = (\omega_{i+1} - \omega_i)(N-1)/d$ respectively. The resulting expression is

$$G_N = (k_{11}/2d)\sum_{i=1}^{N-1}\Big[(\cos^2\theta_i + k_b\sin^2\theta_i)(\theta_{i,z})^2(N-1)$$
$$\cos^2\theta_i(k_t\cos^2\theta_i + k_b\sin^2\theta_i)(\Omega_{i,z})^2(N-1)$$
$$+2k_t(\pi d/\lambda)\cos^2\theta_i\;\Omega_{i,z}\Big]$$
$$-\frac{U^2\varepsilon_0\Delta\varepsilon}{2\kappa d\sum_{i=1}^{N-1}\frac{1}{(N-1)(1+\kappa\sin^2\theta_i)}} \qquad (2)$$
$$+2\gamma_1\sin^2\theta_S + 2\gamma_2\cos^2\theta_S\sin^2(\Phi/2-\Omega_S)$$

where $\Theta_S=\Theta_1=\Theta_N$, $\Omega_S=\Omega_1=\Omega_N$. In order to find the minimum of this function, the values θ_i and ω_i are successively varied. The new orientation is accepted if it leads to the decrease of the total free energy. By repeating such variations, an iterative process is created. It results in the set of N pairs of the angles θ_i and ω_i, that are due to the equilibrium state of the discrete model of the system. If N is sufficiently high, then the values θ_i and ω_i yield the good approximation of the actual continuous director distribution in the layer.

RESULTS AND DISCUSSION

The results for various sets of parameters are presented in Figure 1. The plots of the angles θ_{max} and ψ as functions of the reduced voltage $u=U/[\pi(k_{11}/\varepsilon_0\Delta\varepsilon)^{1/2}]$ show some possible transitions between the twisted and the homeotropic states characterized by the threshold voltages u_1 and u_2 respectively. All the previous catastrophe theory predictions[1] are qualitatively confirmed, although only six examples are presented here. The continuous (Figures 1a, 1e, 1f) and discontinuous (Figures 1b, 1c, 1d) transitions can be found. The director semiprofiles across the layer are also plotted. (The function $\theta(z)$ is even, whereas $\omega(z)$ is odd.) The director orientations are illustrated by means of the set of cylinders positioned at the proper angles. The tilt out of the (xy) plane is maximum in the middle of the layer. The changes of the azimuthal angle have the opposite signs in two halves of the layer. Both types of deformations take place at the boundaries due to the weakness of the anchoring.

The director distribution in the deformed state depends on the relation between the elastic constants and the anchoring energy. In relatively stiff liquid crystal, the director orientation changes almost uniformly in the whole layer under the action of the electric field (Figures 1d, 1e, 1f). In the opposite case, when the material is

(a)

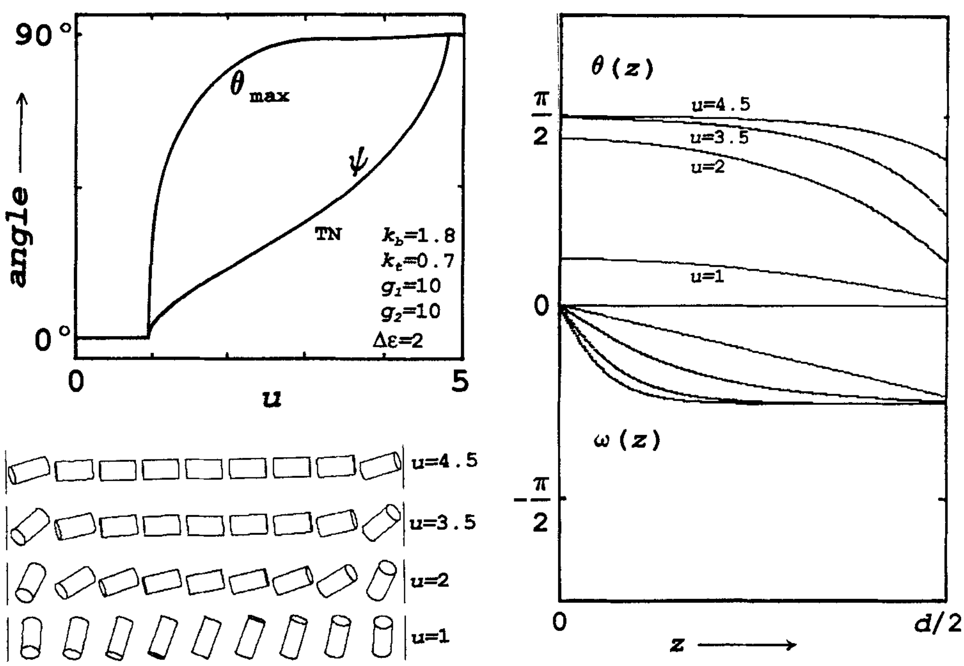

FIGURE 1 The transitions between the twisted and the homeotropic states. See the text for details. $g_{1,2}=\gamma_{1,2}d/k_{11}$, $\varepsilon_\perp=7$, $d/\lambda=-\Phi/\pi$. The other parameters are as indicated.

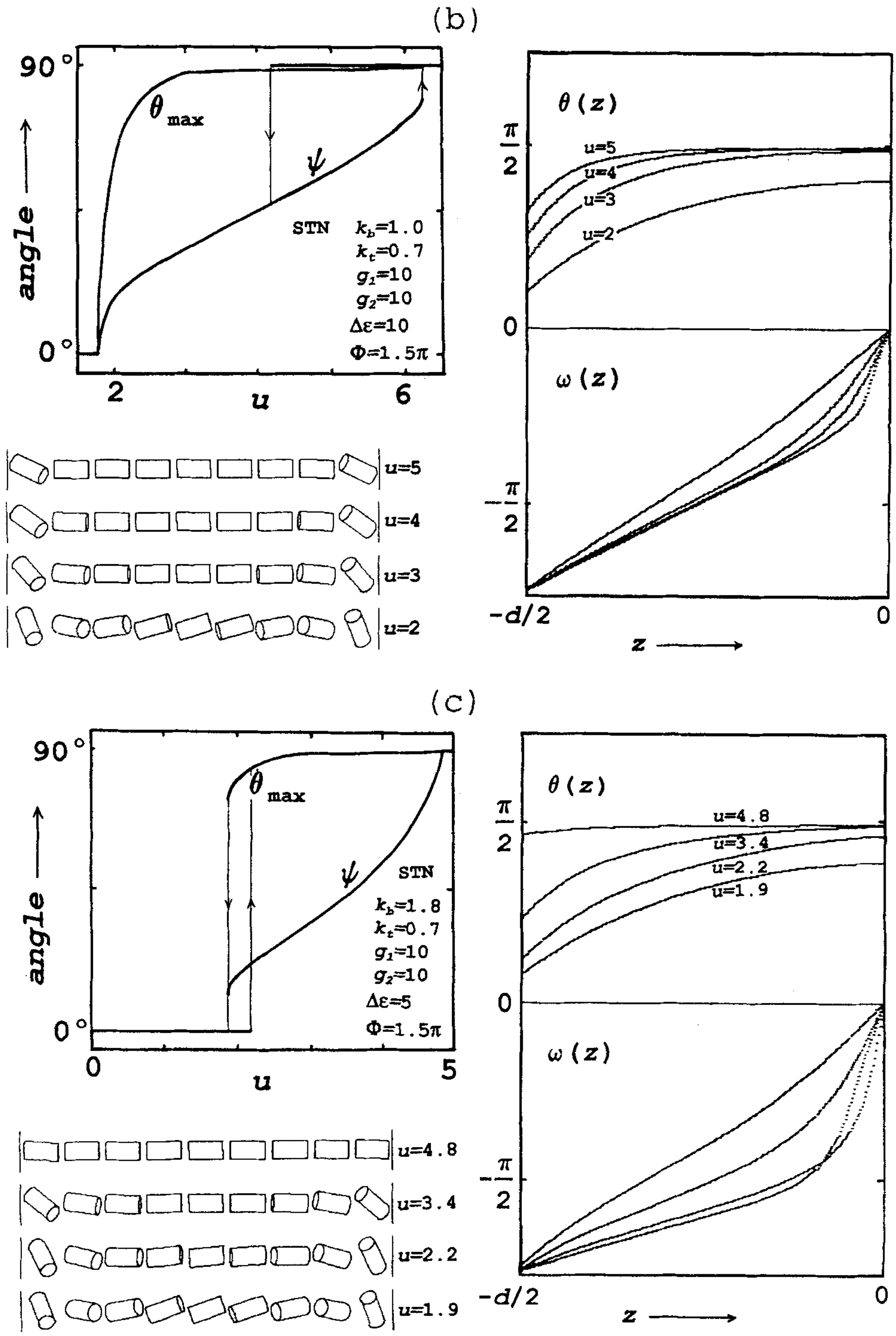

Figure 1 continued.

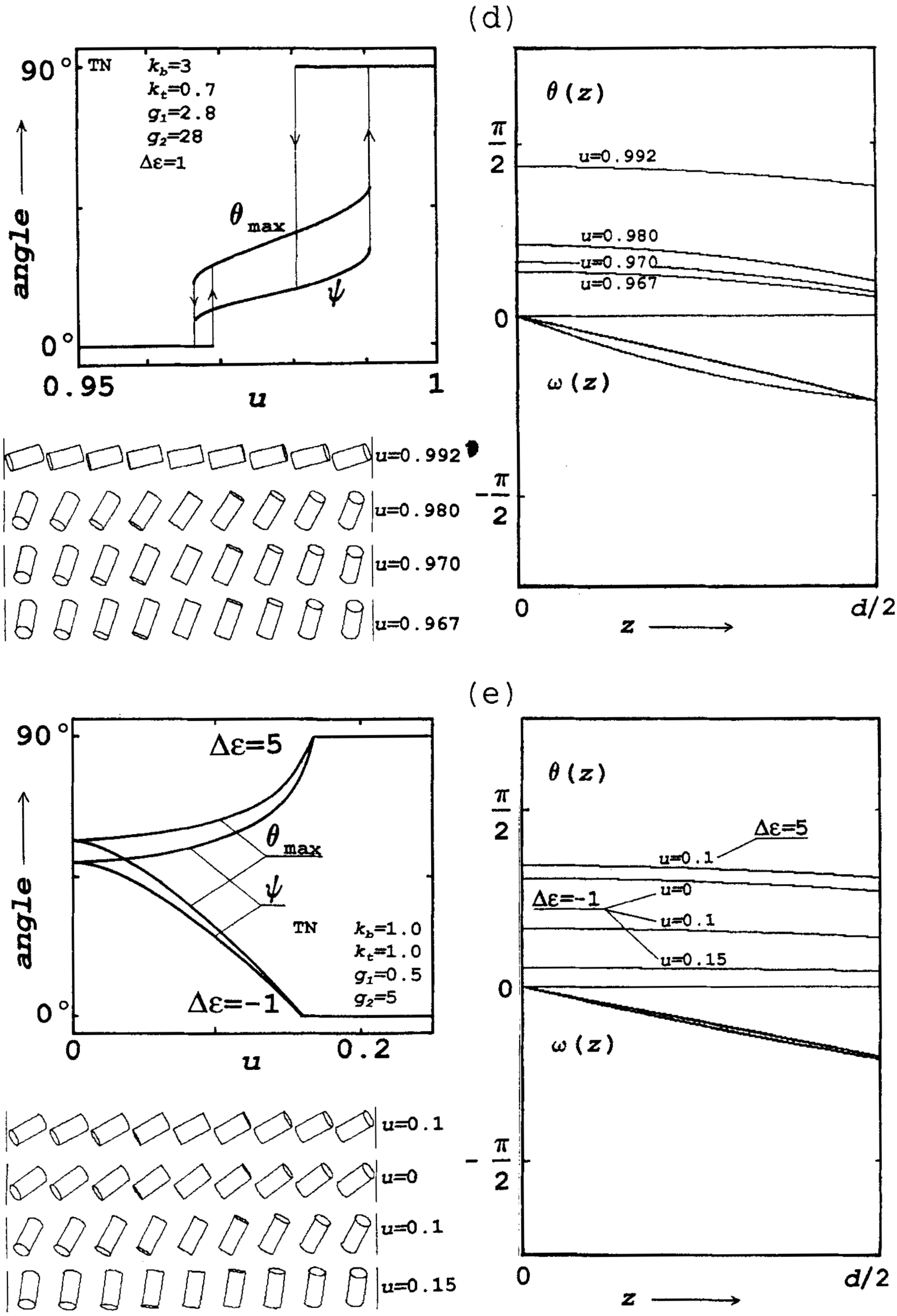

Figure 1 continued.

(f)

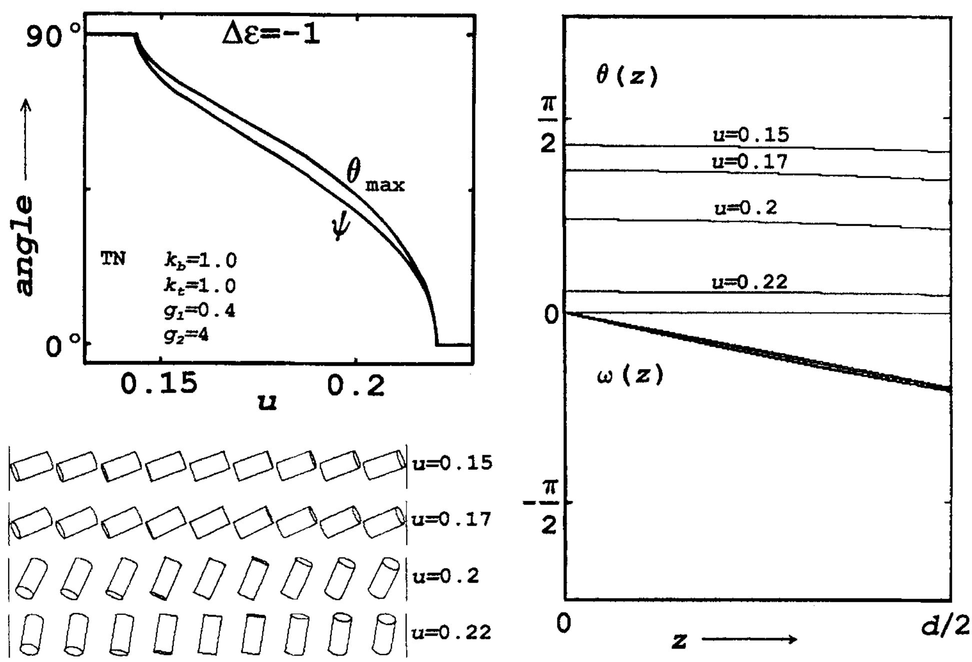

Figure 1 continued.

"soft" in relation to the anchoring, the distribution is highly non-uniform (Figures 1a, 1b, 1c).

The Figures 1a and 1b present the results for the twisted and supertwisted layers. The difference manifests itself only at low voltages. Above $u \cong 3$, the curves $\theta_{max}(u)$, $\psi(u)$ and $\theta(z)$ are very similar. Since the director in the central part of the layer is almost perpendicular to the (xy) plane, the actual value of ω in this region is not important. The layers with $\Phi=1.5\pi$ and with $\Phi=0.5\pi$ behave in the same way.

Figure 1e shows the behaviour of the rather weakly anchored nematic. The structure is deformed in the absence of the field. The transitions to the twisted or homeotropic states, for $\Delta\varepsilon<0$ and $\Delta\varepsilon>0$ respectively, are possible. For somewhat weaker anchoring, the homeotropic state becomes stable without field, as shown in Figure 1f. The transition to the twisted state occurs if $\Delta\varepsilon<0$.

The threshold values calculated earlier[1] are confirmed in most cases. However some differences concerning the u_2 values are noticed (Figures 1a, 1c), when the higher order Fourier components in $\omega(z)$ remain significant in the vicinity of the homeotropic state. They cause the qualitative difference from the term proportional to $\sin(2\pi z/d)$ used in the catastrophe theory approach.

The numerical simulation used here has universal applicability. However, in the vicinity of the thresholds, its effectiveness decreases. The accuracy of the method depends on N. For N=65, the approximate error is about 0.001rad. The corrections introduced by doubling N do not exceed this value.

Application of both methods mentioned in this paper allows to join their advantages effectively. The general review of the possible stationary states, given by the catastrophe theory method, helps to choose the interesting cases, that can be easily treated by the numerical simulation.

REFERENCES

1. G. Derfel, Liquid Crystals, in print.
2. E. Bedford and A. H. Windle, Liquid Crystals, 15, 31 (1993).